12th IEA Heat Pump Conference 2017

.4.5.3Dynamic modelling of an air-cooled LiBr-H_2O absorption chiller based on heat and mass transfer empirical correlations

Joan Farnós[a,b]*, Giorgos Papakokkinos[b], Jesús Castro[b], Sergio Morales[a], Assensi Oliva[b]

[a]*Termo Fluids S. L., Magí Colet 8, 08024 Sabadell (Barcelona), Spain*
[b]*Centre Tecnològic de Transferència de Calor (CTTC), Universitat Politècnica de Catalunya (UPC), ETSEIAT, C. Colom 11, 08222 Terrassa (Barcelona), Spain*

Abstract

The paper describes the numerical modelling of a direct air-cooled single-effect absorption chiller and validates the obtained results by means of experimental data obtained from an own-designed and commissioned small capacity absorption chiller. This direct air-cooled single-effect absorption machine is conceived for low temperature driven, such as solar cooling or waste heat. For performing numerical simulations, a modular object-oriented simulation platform is used (NEST platform tool), which allows the linking between different components (solar collectors, pump, valves, heat exchangers, absorption chiller, etc.). This modelling put in relevance valuable information for further regulation and control protocols. In this numerical platform each component is an object of an arbitrary complexity, which can be either an empirical-based lumped model (e. g. heat exchangers, valves, pumps, etc.) or a detailed 3D CFD calculation if necessary. A lumped parametric dynamic model based on mass, momentum and energy balances, applied to the internal components of the absorption machine (absorber, generator, condenser, evaporator and solution heat exchanger) has been implemented. Thermal and mass storage in each one of the components are taken into account in the transient evaluation and pressure losses in the solution heat exchanger are evaluated by means of a resistance coefficient. The model depends on heat and mass transfer coefficients, which has been implemented depending on basic empirical correlations. The aim of this paper is to improve the available numerical modelling approaches by analyzing the heat & mass transfer phenomena based on previous experiences in falling film absorption. As a first step the model is validated against the results of a previous laboratory prototype. Finally, the performance of a prototype demonstration 7 kW air-cooled LiBr-H_2O absorption chiller is calculated.

Selection and/or peer-review under responsibility of the organizers of the 12th IEA Heat Pump Conference 2017.
Keywords: Absorption, H_2O-LiBr, air-cooled, dynamic simulation

1. Introduction

In the last years there is a renewed interest of sorption systems due to the policy reductions of CO_2 emissions, which leads to the more efficient distributed model of energy production. In this distributed model, sorption systems could play an important role. Small capacity systems (less than 30 kW) could be an interesting option in the present situation. There have been many industrial developments in the last decade mainly in Europe, USA and China. In fact, numerous systems are installed so that many companies had been working in this field. Absorption and adsorption are the main dominant technologies utilized for cooling purposes. Significant companies that have an important role into the market are: i) **Absorption**: York, Carrier, Trane, Broad, Ago, Thermax, Phoenix, Yazaki, Sanyo-McQuay, Entropie, Robur, Pink, ClimateWell, EAW-Shucco, Sonnenklima

* Corresponding author. Tel.: +34-93-739-8066; fax: +34-93-739-8920;
E-mail address: joan@termofluids.com

and Rotartica (not available); ii) **Adsorption**: Nishyodo, Mayekawa, Sortech, SJTU, Invensor, SolabCool. There are other developments in an earlier stage [1-6].

Within the design stage it is interesting to use thermodynamic models [7] due to, especially in commercial units, the fact that internal parameters are not available. This kind of modelling requires a wide range of parameters such as experimental overall heat transfer coefficients, flow rates of solution, properties of the working fluids, etc. However, in the last years dynamic simulation has been approached by several authors aiming to design and improve different LiBr-H_2O absorption cycles. Monitoring the real performance of a thermal device in transient conditions allows to understand the behaviour of the chiller under part-load, full load and critical operation procedures such as the activation or turning off the chiller.

A large number of numerical models for the simulation of the entire absorption machine have been published in the literature. Scientific community has aimed to simulate the transient performance of an absorption chiller. Anand et al. (1982) [8] presented a study related to the chiller start-up, where the modelisation of the transient behaviour of the chiller was the goal of the paper, Jeong et al [9] presented a dynamic numerical simulation to predict the transient operating characteristics and performance of an absorption heat pump recovering low grade waste heat. A. Joudi et al. [10] presented a model based on detailed mass and energy balances and heat and mass transfer relationships. Kohlenbach and Ziegler [11] presented an enthalpy based internal and external analysis to carry dynamic simulations. Arora et al. [12] developed a computational model for the parametric investigation of single-effect and series flow double-effect LiBr/H_2O absorption refrigeration systems. Shin et al. [13] developed a dynamic model to simulate dynamic operation of a commercial double-effect absorption chiller. Bittanti et al. [14] also presented a dynamic model of an absorption chiller for air-conditioning. Matsushima (2010) [15] based the numerical modelling approach on an object-oriented numerical platform. A new dynamic simulation program for predicting the transient behavior of absorption chillers with arbitrary cycle configurations was developed. This program combined an object-oriented formulation and parallel processing program architecture. Mirzaei [16] presented a transient modelling of a double-effect absorption chiller based on lumped parameters. Iranmanesh [17] developed a lumped-parameter dynamic simulation of a single-effect LiBr-H_2O absorption chiller. That study considered the effect of quality on the concentration of solution at the outlets of generator and absorber and then the effect of thermal masses. Zinet et al. [18] presented a dynamic model for the simulation of a new single-effect LiBr/H_2O absorption chiller. Heat and mass transfer in the evaporator–absorber and in the desorber are described according to a physical model for vapour absorption based on Nusselt's film theory. The other heat exchangers are treated using a simplified approach based on the NTU-effectiveness method. Evola et al. [19] proposed and validated a model for the dynamic simulation of a solar-assisted single-stage LiBr/water absorption chiller (2013). More recently Marc et al. [20] analysed the transient and steady state phases behaviour of the LiBr/H_2O of a single effect absorption chiller, modelled accurately using a dynamic model presented.

The aim of this research is to develop a low capacity (7kW) single-effect air-cooled absorption chiller. The dynamic model has been conceived as a powerful tool both for thermal design and complete understanding of the system under several operating conditions. This dynamic model was already implemented on an object-oriented numerical platform called NEST [21-23], and now several modifications have been performed in the model mainly in the mass transfer calculations in order to improve the accuracy and reliability. The dynamic model has been validated against the experimental results of a previous research performed with a laboratory prototype of an air-cooled absorption machine (Castro et al. 2007, 2008) [24-25]. Then, dynamic capability is showed in a sequence of operation by switching between three operation modes of the prototype. Finally, the nominal performance of the new pre-industrial prototype is calculated with the validated model.

Table 1. Nomenclature

Name	***Description***	***Units***	***Greek symbols***	***Description***	***Units***
A	Heat exchanger area	m^2	α	Heat transfer coefficient	$Wm^{-2}K^{-1}$
c	LiBr weight concentration	-	δ	Film thickness	m
C_d	Discharge coefficient	-	Γ	Liquid flow rate per unit length	$Kgm^{-1}s^{-1}$
c_p	Heat capacity	$Jkg^{-1}K^{-1}$	λ	Thermal conductivity	$Wm^{-1}K^{-1}$

d	Outer diameter of the tube	m	μ	Dynamic viscosity	Pa·s
D	Mass diffusivity	m^2s^{-1}	ν	Kinematic viscosity	m^2s^{-1}
g	Gravitational acceleration	ms^{-2}	ρ	Density	kgm^{-3}
F	Fouling factor	m^2KW^{-1}	ζ	Pressure drop coefficient	-
h	Specific enthalpy	Jkg^{-1}	***Subscripts & Superscripts***	***Description***	
H	Height between components	m	A	Absorber	
j	Colburn factor	-	abs	Absorbed	
k	Overall mass transfer coefficient	ms^{-1}	air	Air side	
L	Characteristic length	m	amb	Ambient	
$\dot{m}$	Mass flow	kgs^{-1}	b	Bulk	
M	Mass	Kg	C	Condenser	
p	Pressure	Pa	cond	Condensed	
p_d	Fin amplitude	m	des	Desorbed	
p_l	Vertical distance between tubes	m	E	Evaporator	
p_t	Horizontal distance between tubes	m	evap	Evaporated	
Pr	Prandtl number	-	i	Interface	
R	Thermal resistance	WK^{-1}	in	Inlet	
Re	Reynolds number	-	f	Film	
R_v	Specific gas constant	$Jkg^{-1}K^{-1}$	G	Generator	
s	Distance between fins	m	hx	Heat exchanger	
S	Pipe section between components	m^2	l	liquid	
Sc	Schmidt number	-	loss	Losses	
Sh	Sherwood number	-	out	Outlet	
St	Stanton number	-	pri	Primary	
t	Time	S	s	Solution	
T	Temperature	K	sec	Secondary	
U	Overall heat transfer coefficient	$Wm^{-2}K^{-1}$	v	Vapour	
v	Velocity	ms^{-1}	t	Tube	
V	Volume	m^3	w	Wall	
x	LiBr molar concentration	-	*	Dimensionless	
x_f	Half-length wave of the fin	m			
z	Liquid level in component	m			

1. Mahematical modelling

The system to be simulated is a single-effect H_2O-LiBr absorption cycle. Figure 1 shows a schematic representation. For each component, overall balances of mass, species and energy have been established under

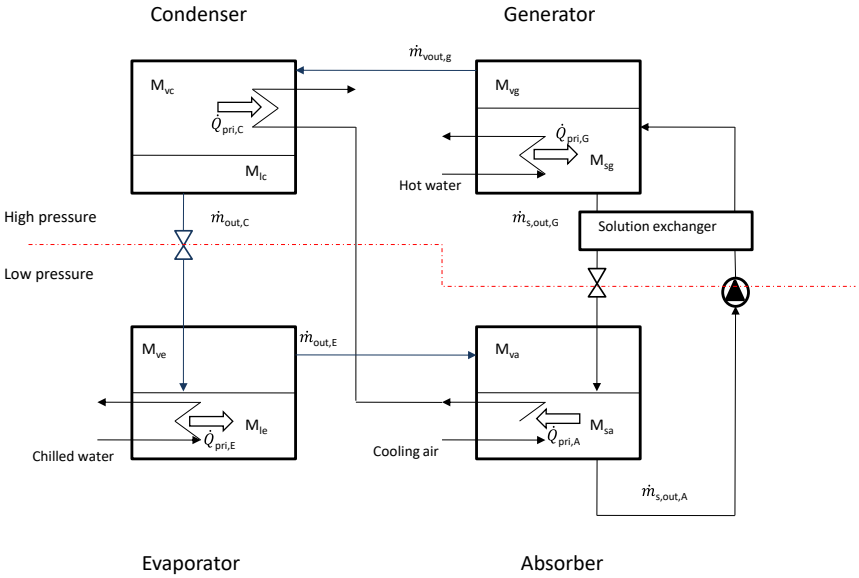

transient conditions. In order to close the system, momentum balance has been assumed for the two expansion valves.

Fig. 1. Schematic representation of the single effect, air-cooled LiBr-H_2O absorption cycle

1.1. Equations

The equations for the generator are the following:

$$\dot{m}_{s,in,G} - \dot{m}_{s,out,G} - \dot{m}_{v,des} = \frac{dM_{s,G}}{dt} \quad (1)$$

$$\dot{m}_{v,des} - \dot{m}_{v,out,G} = \frac{dM_{v,G}}{dt} \quad (2)$$

$$M_{v,G} R_v T_G = p_G V_v \quad (3)$$

$$V_v = V_G - M_{s,G} / \rho_{s,G} \quad (4)$$

$$\dot{m}_{s,in,G} c_{s,in,G} - \dot{m}_{s,out,G} c_{s,out,G} = M_{s,G} \frac{dc_{s,G}}{dt} + c_{s,G} \frac{dM_{s,G}}{dt} \quad (5)$$

$$\dot{Q}_{pri,G} - \dot{Q}_{loss,G} = \dot{m}_{v,des} h_{v,des} + \dot{m}_{s,out,G} h_{s,out,G} - \dot{m}_{s,in,G} h_{s,in,G} + M_{s,G} c_{p,s,G} \frac{dT_{s,G}}{dt} + u_{s,G} \frac{dM_{s,G}}{dt} \quad (6)$$

$$\dot{m}_{s,out} = C_d S \sqrt{\frac{2\rho_s (p_G - p_A) + \rho_s g (H + z)}{\zeta}} \quad (7)$$

$$\dot{m}_{v,des} = k_{des} A \rho_s \frac{1}{2} \left(\frac{1}{x_{in,i}} \ln\left(x_{in,b} / x_{in,i}\right) + \frac{1}{x_{out,i}} \ln\left(x_{out,b} / x_{out,i}\right) \right) \quad (8)$$

Where eq. (1) is mass balance in the liquid solution phase, eq. (2) the mass balance in vapour phase, eq. (3) the state equation of the vapour (ideal gas is assumed), eq. (4) is the volume balance in the generator, eq. (5) is the LiBr balance in the liquid solution phase, eq. (6) is the energy balance in the liquid solution phase, eq. (7) is the momentum balance at the generator-absorber line and eq. (8) is the calculation of the mass transfer rate. The equations for the absorber are:

$$\dot{m}_{s,in,A} - \dot{m}_{s,out,A} + \dot{m}_{v,abs} = \frac{dM_{s,A}}{dt} \quad (9)$$

$$\dot{m}_{v,in,A} - \dot{m}_{v,abs} = \frac{dM_{v,A}}{dt} \quad (10)$$

$$M_{v,A} R_v T_A = p_A V_v \quad (11)$$

$$V_v = V_A - M_{s,A} / \rho_{s,A} \quad (12)$$

$$\dot{m}_{s,in,A} c_{s,in,A} - \dot{m}_{s,out,A} c_{s,out,A} = M_{s,A} \frac{dc_{s,A}}{dt} + c_{s,A} \frac{dM_{s,A}}{dt} \quad (13)$$

$$\dot{Q}_{pri,A} - \dot{Q}_{loss,A} = \dot{m}_{s,out,A} h_{s,out,A} - \dot{m}_{s,in,A} h_{s,in,A} - \dot{m}_{v,abs} h_{v,abs} + M_{s,A} c_{p,s,A} \frac{dT_{s,A}}{dt} + u_{s,A} \frac{dM_{s,A}}{dt} \quad (14)$$

$$\dot{m}_{v,abs} = k_{abs} A \rho_s \frac{1}{2} \left(\frac{1}{x_{in}} \ln\left(x_{in,b} / x_{in,i}\right) + \frac{1}{x_{out}} \ln\left(x_{out,b} / x_{out,i}\right) \right) \quad (15)$$

Where eq. (9) is mass balance in the liquid solution phase, eq. (10) the mass balance in vapour phase, eq. (11) the state equation of the vapour (ideal gas is assumed), eq. (12) is the volume balance in the absorber, eq. (13) is the LiBr balance in the liquid solution phase, eq. (14) is the energy balance in the liquid solution phase and eq. (15) is the calculation of the mass transfer rate. The equations for the condenser are the following

$$\dot{m}_{cond} - \dot{m}_{l,out,C} = \frac{dM_{l,C}}{dt} \quad (16)$$

$$\dot{m}_{v,in,C} - \dot{m}_{cond} = \frac{dM_{v,C}}{dt} \quad (17)$$

$$\dot{Q}_{pri,C} - \dot{Q}_{loss,C} = \dot{m}_{cond} h_{l,out} - \dot{m}_{v,in,c} h_{v,in,C} + M_{v,C} c_{p,v,C} \frac{dT_{v,c}}{dt} + u_{v,C} \frac{dM_{v,C}}{dt} \quad (18)$$

$$\dot{m}_{l,out,C} = C_d S \sqrt{\frac{2\rho_s (p_G - p_A) + \rho_s g(H+z)}{\zeta}} \quad (19)$$

Where eq. (16) is mass balance in the liquid solution phase, eq. (17) the mass balance in vapour phase, eq. (18) is the energy balance in the vapour phase and eq. (19) is the momentum balance at the condenser-evaporator line. For the evaporator the equations are:

$$\dot{m}_{l,in,E} - \dot{m}_{evap} = \frac{dM_{l,E}}{dt} \quad (20)$$

$$\dot{m}_{evap} - \dot{m}_{v,out,E} = \frac{dM_{v,E}}{dt} \quad (21)$$

$$\dot{Q}_{pri,E} - \dot{Q}_{loss,E} = \dot{m}_{v,out,E} h_{v,out,E} - \dot{m}_{l+v,in,E} h_{l+v,in,E} + M c_{p,l,E} \frac{dT_{l,E}}{dt} + u_{l,E} \frac{dM_{l,E}}{dt} \quad (22)$$

Where eq. (20) is mass balance in the liquid solution phase, eq. (21) the mass balance in vapour phase and eq. (22) is the energy balance in the liquid.

For the calculation of the heat exchangers the following energy balance is performed at the solid part:

$$M_{hx} c_{p,hx} \frac{dT_{hx}}{dt} = \dot{Q}_{\sec} - \dot{Q}_{pri} \quad (23)$$

Where the heat at the primary and secondary streams are calculated in the following way, respectively:

$$\dot{Q}_{pri} = (UA)_{pri} (T_{in,pri}/2 + T_{out,pri}/2 - T_{hx}) \quad (24)$$

$$\dot{Q}_{\sec} = \left[1 - \exp(-UA_{\sec}/(\dot{m}_{\sec} c_{p,\sec}))\right] \dot{m}_{\sec} c_{p,\sec} (T_{in,\sec} - T_{hx}) \quad (25)$$

The concentrated solution rate (see eq, 7) is obtained by adapting the expression described by Evola et al. [19] or Köhlenbach and Ziegler [11] in order to overcome the possibility of emptying the desorber or the condenser. This expression is highly dependent on the ζ which value is a function of piping and solution heat exchanger in the case of desorber .Therefore, it is important to obtain manufacturing characteristics. Moreover, ζ is recalculated at each time step depending on the total amount of liquid at the vessels, which is permanently controlled in order to avoid emptied vessels and to analyse the thermal inertia of accumulated terms. On the other hand, volumetric flow is imposed constant according to solution pump characteristics.

The mass transfer rates at the generator and absorber, eqs. (8) and (15), respectively, are calculated by means of basic empirical information on mass transfer coefficients [26][27]. In these expressions, the mass transfer is related with respect to the basic concentration difference assuming unidirectional mass transport. In order to calculate in an accurate way the heat and mass transfer rates at the interface, LiBr concentrations and temperatures at the interface have been defined (c_i, T_i), and the heat at the interface is related to the mass transfer at the interface by means of the following relation (for both generator and absorber), assuming thermodynamic equilibrium conditions:

$$\alpha_i (T_b - T_i) = \dot{m}_{des/abs} \Delta h_{des/abs}, \; T_i = f(c_i, p) \quad (26)$$

Where the heat transfer coefficient at the interface (α_i) is calculated by means of a Nu/Sh analogy [28] and the equilibrium relation has been calculated from McNeely [29].

1.2. Numerical resolution

As commented, the proposed mathematical model is based on the transient resolution of the different components of the absorption machine. The integration of the different components is carried out by means of a modular object-oriented tool named NEST [23]. Each component is treated as a different object coupled with its neighbour objects/elements through a global algorithm based on an implicit iteration of each component. At each iteration, inputs (e.g., pressure, temperature, etc.) are taken from the neighbours, governing equations of the element are solved and the outputs (e.g., pressure, temperature, etc.) are set as boundary conditions for the resolution of the neighbour elements. Iterations continue until convergence is reached at the present time step and then the next time step calculation starts after updating the variables in Gauss-Seidel iteration procedure.

2. Results

2.1. Validation based on previous steady state results

Table 2. Parameters of the validation case

Component	UA_{int} (W/K)	UA_{ext} (W/K)	k (m/s)	$\dot{m}$ (kg/s)
Generator	425	4900	2.0e-4	0.10
Absorber	2050	1500	1.5e-4	0.92
Condenser	12600	1400	-	0.92
Evaporator	940	1830	-	0.07
SHX	290 (overall value)		-	0.046

Experimental data have been reviewed and obtained from [24-25]. In order to validate the dynamic model for this device, the authors have considered this 2 kW air-cooled machine where it is possible to understand and design strategies of regulation and control. This chiller was tested at the laboratory of the Heat and Mass Transfer Technological Center at the Technical University of Catalonia (UPC). Each case has been simulated in a transient mode until the steady state is reached. The U and k values have been calculated from the empirical relations explained at the appendix (see Table 2).

In the next figures (from 2 to 5) the comparison of COP (defined as $COP = \dot{Q}_E/\dot{Q}_G$) and cooling capacity is shown. It can be observed the close accuracy in the COP estimation. For the case of the capacity ($\dot{Q}_E$), there is a slight underestimation of the values, up to 15%. A possible explanation is the calculation of the U and k values under nominal working conditions, values that are maintained as constant during all the calculations.

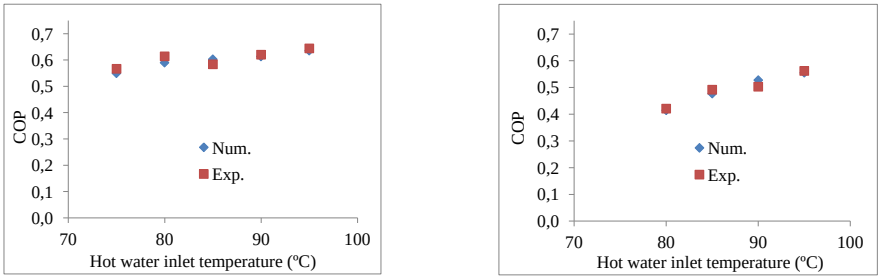

Fig. 2. COP vs. hot water inlet temperature ($T_{sec,in,G}$) of validation case for output chilled water at 9ºC. Left, ambient air at 30ºC, right ambient air at 35ºC.

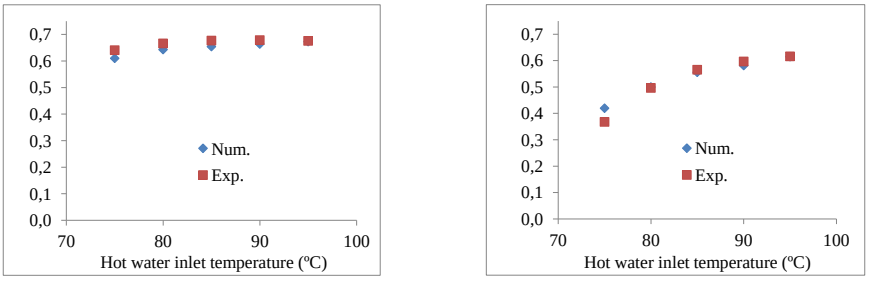

Fig. 3. COP vs. hot water inlet temperature ($T_{sec,in,G}$) of validation case for output chilled water at 12ºC. Left, ambient air at 30ºC, right ambient air at 35ºC.

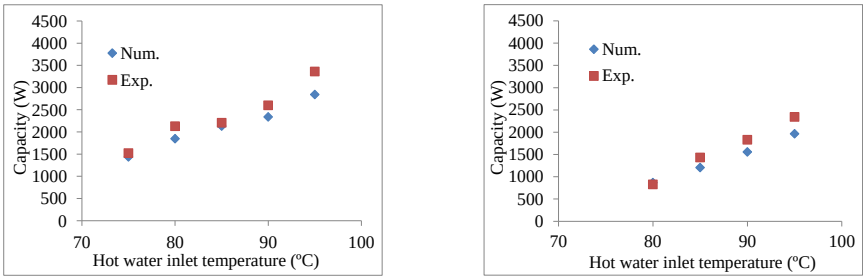

Fig. 4. Capacity (W) vs. hot water inlet temperature ($T_{sec,in,G}$) of validation case for output chilled water at 9ºC. Left, ambient air at 30ºC, right ambient air at 35ºC.

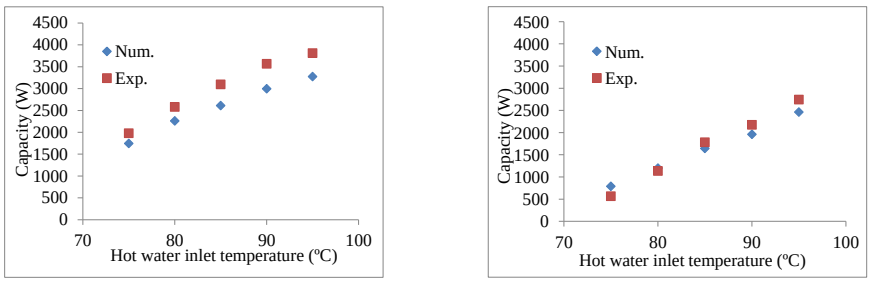

Fig. 5. Capacity (W) vs. hot water inlet temperature ($T_{sec,in,G}$) of validation case for output chilled water at 12ºC. Left, ambient air at 30ºC, right ambient air at 35ºC.

2.2. Example on transient process

In order to show the capabilities of the transient simulation, a sequence of operation has been simulated for the laboratory prototype. The sequence starts at the conditions indicated at Table 3. Then, the input hot water temperature $T_{sec,in,G}$, changes from 85ºC to 95ºC (2nd stage of the transient simulation), and finally, when de ambient temperature decreases from 35ºC to 30ºC, the inlet hot water temperature $T_{sec,in,G}$, also decreases from 95ºC to 75ºC. Each stage of the simulation lasts 3600 s, and the time step used is Δt = 1e-2 s. Figures 6 and 7 shows the evolution of the main parameters of the cycle: pressures, temperatures, LiBr concentrations and liquid mass inside the shells.

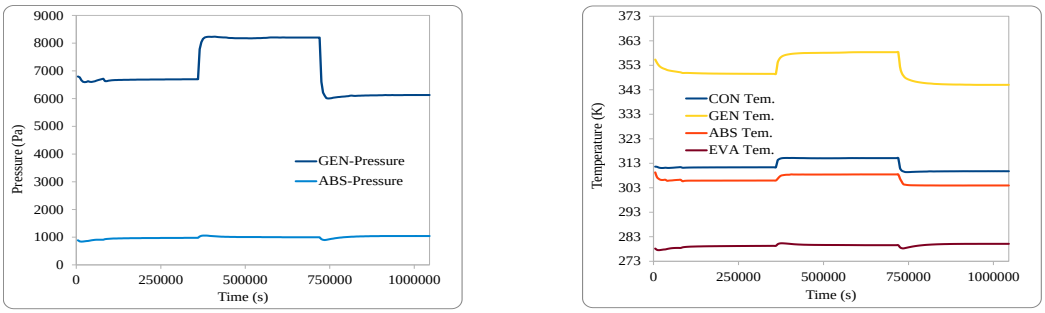

Fig. 6. Left, evolution of the pressure levels (Pa); right, evolution of the main temperatures of the absorption machine (K)

Fig. 7. 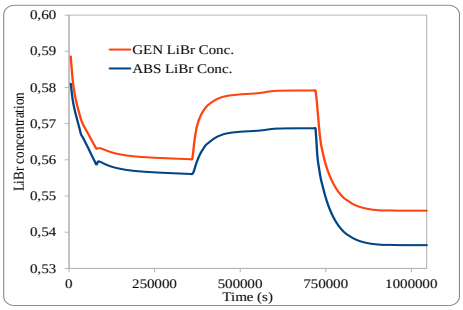

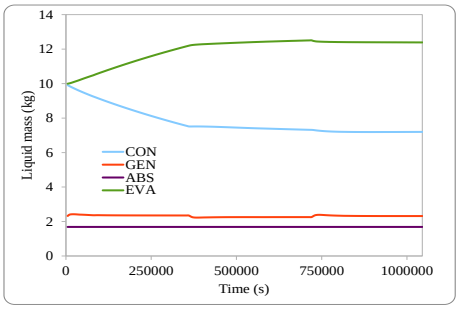

Left, evolution of the LiBr concentration levels; right, evolution of the liquid mass inside the shells of the absorption machine (kg)

With this dynamic model it will be possible in the future to simulate the thermally driven chiller under different control strategies, start/stop procedures, etc., with the objective to maximize the seasonal performance (e. g. solar cooling installations) of the machine and avoiding crystallization.

2.3. Prediction of the performance of the pre-industrial prototype

Table 3. Parameters of the prototype demonstration

Component	UA_{int} (W/K)	UA_{ext} (W/K)	k (m/s)	$\dot{m}$ (kg/s)
Generator	1890	12900	9.3e-4	0.48
Absorber	4400	3540	4.7e-4	1.86
Condenser	12600	1885	-	1.06
Evaporator	4090	14300	-	0.33
SHX	1580 (overall value)		-	0.095

Once the model has been validated, it is used to predict the performance of a prototype demonstration that is being set-up at the UPC-CTTC facilities. The nominal capacity expected is 7 kW, according to the initial design of the heat exchangers. Table 3 summarizes the main thermal parameters of the demo-prototype.

According to these design parameters it is expected a capacity of about 5.7 kW with a COP of 0.75 at nominal working conditions: $T_{sec,in,G}$ = 85ºC, T_{amb} = 35ºC, $T_{sec,in,E}$ = 14ºC, therefore it has been achieved the 81% of the nominal capacity expected.

3. Conclusions

In this work a dynamic model for an air-cooled H_2O-LiBr absorption machine is presented. The model is based in the use of heat & mass transfer empirical correlations of the scientific literature, to avoid ad-hoc adjusts of the main parameters of the absorption refrigeration cycle. The calculation of the heat & mass transfer parameters of the model has been validated with previous steady state experimental results of a laboratory prototype of 2-3 kW of cooling capacity with a reasonable agreement in the COP values, being capacity slight under predicted. With

this dynamic transient capability of the model, it is expected in the future to simulate the absorption chiller under different control strategies and full start/stop processes.

Finally, the model has been used to predict the future performance of a prototype demonstration that is being developed at the UPC-CTTC facilities. Although the heat exchangers have been designed to provide a nominal capacity of 7 kW, the model predicts about the 81% of the cooling capacity expected (5.7 kW).

Acknowledgements

This research has been financed and supported by the Spanish Government through the project: "Modelización multiescala y simulación numérica directa de flujos multifásicos gas líquido en burbujas, películas y esprays." (Ref. ENE2015-70672-P) and through the Program *Torres Quevedo* of the Ministerio de Economía y Competitividad.

APPENDIX

This appendix summarizes the correlations used in the calculation of the thermal size of the heat exchangers (UA) and the mass transfer coefficients (k) presented in table 2 and table 3. Using Hobler's criterion [30] UA and k have been calculated with more accuracy taking into account the wetting area.

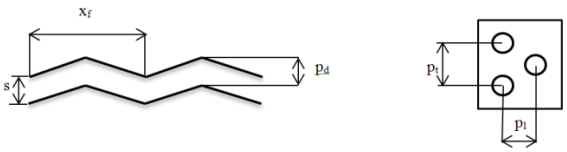

According to the dimensionless analysis Schmidt number, Prandtl number, Reynolds number, Nusselt number, Stanton number are defined as follows: $Sc = \frac{\mu l}{\rho D}$; $Pr = \frac{\mu c_p}{\lambda}$; $Re_f = \left(\frac{4\Gamma}{\mu}\right)$; $Re_{air/tub} = \rho v L/\mu$; $Nu = \frac{\alpha \cdot L}{\lambda}$; $St = \frac{\alpha}{\rho v d}$

Primary circuit **absorber** [32]: $\alpha = 0.029 \cdot (4Re_f)^{0.53} Pr^{0.344} \frac{\lambda}{\delta}$; $k = 0.7\sqrt{D}\left(\frac{\left(\sqrt{g}\left(\frac{4\Gamma}{\mu}\right)\right)}{2000\sqrt{\delta}}\right)^{1/2}$ *(27)*

Primary circuit **condenser,** estimated values have been considered according to [31].

Primary circuit **desorber** [27]: $d^* = d/L; = (\nu^2/g)^{1/3}$; $Nu = 0.7893 \cdot Re_f^{0.16587} \cdot Pr^{0.37275} \cdot Sc^{-0.041769} \cdot d^{*-0.40335}$; $Sh = 0.0020 Re_f^{1.0023} Pr^{-0.74049} Sc^{1.3455} d^{*-1.0006}$ *(28)*

In this work, the mass transfer rate is adapted by using a different logarithmic difference of the LiBr-Water concentration is spite of a simple temperature difference as is [27].

Primary circuit **evaporator**: For the falling film evaporator the calculation of the heat transfer coefficient is based on [32]:

$$\alpha = 0.821 \cdot \left(\frac{\nu^2}{\lambda^3 \cdot g}\right)^{-1/3} \left(\frac{4\Gamma}{\mu}\right)^{-0.22} \quad (29)$$

For further details regarding the 7kW flooded evaporator heat transfer calculation see [33].

Secondary stream **Absorber and Condenser** (air side) [34]:

$$j = 0.394 \cdot Re_{air}^{-0.357} \cdot \left(\frac{p_t}{p_l}\right)^{-0.272} \cdot \left(\frac{s}{D}\right)^{-0.205} \cdot \left(\frac{x_f}{p_d}\right)^{-0.558} \cdot \left(\frac{p_d}{s}\right)^{-0.133}; where\ j = St \cdot Pr^{2/3} \quad (30)$$

Secondary stream **desorber and evaporator** [35]:

$$Nu = 0.027 \cdot {Re_{tub}}^{0.8} \cdot Pr^{0.33} \cdot \left(\frac{\mu}{\mu_w}\right)^{0.14} \quad (31)$$

References

[1] Zamora, M., Bourouis M., Coronas, A., and Vallès, M. Pre-industrial development and experimental characterization of a new air-cooled and water-cooled NH_3-$LiNO_3$ absorption chiller. International Journal of

Refrigeration, 45, 189-197, 2014.
[2] Izquierdo, M., González-Gil, A., and Palacios, E. Solar-powered single-and-double effect directly air-cooled LiBr-Water absorption prototype built as a single unit. Applied Energy, 130, 7-19, 2014.
[3] Prasartkaew, B. Performance test of a small size LiBr-Water absorption chiller. Energy Procedia, 56, 487-497, 2014.
[4] Boudéhenn, F., Demasles, H., Wyttenbach, J., Jobard, X., Chèze, D., and Papillon, P. Development of a 5kW cooling capacity NH_3-Water absorption chiller for solar cooling applications. Energy Procedia, 30, 35-43, 2012.
[5] Franchini, G., Notarbartolo, E., Padovan, L.E., and Perdichizzi, A. Modeling Design and Construction of a Micro-scale Absorption Chiller. Energy Procedia, 82, 577–583, 2015.
[6] Xie, Guozhen, Wu, Qingping, Fa, Xiaoming, Zhang, Lirong, Bansal, Pradeep. A novel lithium bromide absorption chiller with enhanced absorption pressure. Applied Thermal Engineering, Vol. 38, 1-6, 2012.
[7] Florides, G.A., Kalogirou, S.A., Tassou, S.A., Wrobel L.C. Design and construction of a LiBr-H_2O absorption machine. Energy Conversion and Management, 44, 2483-2508, 2003.
[8] Anand, D.K., Allan, R.W., and Kumar, B. Transient simulation of absorption machines. Journal of Solar Energy Engineering. 104, 197, 1982.
[9] S. Jeong, B.H. Kang and S. W. Karngt. Dynamic simulation of an absorption heat pump for recovering low grade wasted heat. Applied Thermal Engineering Vol. 18, Nos. 1 2, pp. 1-12, 1998.
[10] Joudi, K.A., and Lafta, Ali H. Simulation of a simple absorption refrigeration system. Energy Conversion and Management. 42, pp 1575-1605, 2001.
[11] Kohlenbach, P., and Ziegler, F. A dynamic simulation model for transient absorption chiller performance. Part I: the model, International Journal of Refrigeration, Vol. 31, pp. 217-225, 2008.
[12] Arora, A. and Kaushick, S.C. Theoretical analysis of LiBr/H_2O absorption refrigeration systems. International Journal of Energy Research. 33, 1321-1340, 2009.
[13] Shin, Y., Seo, J.A., Cho, H.W., Nam, S.C., and Jeong J.H. Simulation of dynamics and control of a double-effect LiBr-H_2O absorption chiller. Applied Thermal Engineering, 29 (13), 2718-2725, 2009.
[14] Bittanti, S., De Marco, A., Giannatempo, M., and Prandoni, V. A Dynamic Model of an Absorption Chiller for Air Conditioning. (ICREPQ'10), Granada (Spain), 2010.
[15] Matsushima, H., Fujiib, T., Komatsub, T., and Nishiguchic, A. Dynamic simulation program with object-oriented formulation for absorption chillers (modeling, verification, and application to triple-effect absorption chiller). International Journal of Refrigeration, 33, 259-268, 2010.
[16] Mirzaei, A., Nouri, A. and Shojaee-Fard, M.H. Transient modelling of a double-effect absorption refrigeration system. 3rd International Conference on Applied Energy, 2011.
[17] Iranmanesh, A. and Mehrabian, M.A. Dynamic simulation of a single-effect LiBr–H_2O absorption refrigeration cycle considering the effects of thermal masses. Energy and Buildings, 60, 47–59, 2013.
[18] Zinet, M., Rulliere, R., Haberschill, P. A numerical model for the dynamic simulation of a recirculation single-effect absorption chiller. Energy Conversion and Management, 62, 51-63, 2012.
[19] Evola, G., Le Pierrès, N., Boudehenm, F. and Papillon, P. Proposal and validation of a model for the dynamic simulation of a solar-assisted single-stage LiBr/water absorption chiller, International Journal of Refrigeration, V. 36, 1015-1028, 2013.
[20] Marc, O., Sinama, F., Praene, J.P., and Lucas, F. Dynamic modelling and experimental validation elements of a 30kW LiBr/H_2O single effect absorption chiller for solar application. Applied Thermal Engineering 90, pp 980-993, 2015.
[21] Farnós, J., Castro, J., Morales, S., García-Rivera, E., and Oliva, A. Preliminary evaluation of a pre-industrial air-cooled LiBr-H_2O small capacity absorption machine. 11th IIR Gustav Lorentzen Conference on Natural Refrigerants, Hangzhou, China, 2014.
[22] Farnós, J., Castro, J., Morales, S., García-Rivera, E., Oliva, A., Kizildag, D. Preliminary results of a pre-industrial air-cooled LiBr-H_2O small capacity absorption machine. EuroSun 2014, Aix-les-Bains, France, 2014.
[23] Lopez J., Lehmkuhl O, Damle R, Rigola J. A parallel and object-oriented general purpose code for simulation of multiphysics and multiscale systems. In: 24th Int. Conference on Parallel CFD, Atlanta; 2012.
[24] Castro J, Oliva A, Perez-Segarra CD, Cadafalch J. Evaluation of a small capacity, hot water driven, air-cooled H_2O–LiBr absorption machine. HVAC&R;13(1):59–75. 2007.
[25] Castro, J., Oliva, A., Pérez-Segarra, C.D. and Oliet, C., Modelling of the heat exchangers of a small capacity, hot water driven, air-cooled H_2O-LiBr absorption cooling machine, International Journal of Refrigeration, 31(1), p. 75-86, 2008.
[26] Seban, R.A. Transport to falling films. International Heat Transfer Conference, 6th, Toronto, Canada, August 7-11, 1978, General Papers. Vol. 6. (A79-43012 18-34) Washington, D.C., Hemisphere Publishing Corp., 417-428, 1978.

[27] Jani, S. Simulation of heat and mass transfer process in falling film single tube absorption generator. International Science and Engineering Investigations, Vol. 1, Issue 3, 79-84, 2012.
[28] Yuksel, M.L. and Schlünder, E.U. Heat and Mass Transfer in non-isothermal absorption of gases in liquid falling liquid films. Part I: Experimental determination of heat and mass transfer coefficients. Chem. Eng. Process, 22, 193-202, 1987.
[29] L. McNeely. Thermodynamic properties of aqueous solutions of Lithium Bromide, ASHRAE Transactions, Vol. 85, Pt.1, 413-434, 1979.
[30] Hobler, T. Minimum surface wetting, Chemia Stosow (1964) 145-159.
[31] Hannemann, R.J. and Mikic, B.B. An experimental investigation into the effect of surface thermal conductivity on the rate of heat transfer in dropwise condensation. International Journal of Heat and Mass Transfer, Vol. 19, 1309-1317.54, 1976.
[32] Chun, K.R. and Seban, R.A.Heat transfer to evaporating liquid films. J. of Heat Transf, 93, 391-396, 1971.
[33] Castro, J., Farnós, J., Oliva, A., García-Rivera, E. Flooded evaporators for LiBr-Water absorption chillers: Modelling and validation. 8th IIR Gustav Lorentzen Conference on Natural Refrigerants, Copenhagen, 2008.
[34] N.H. Kim, J.H. Yun, R.L. Webb, Heat transfer and friction correlations for wavy plate fin-and-tube heat exchangers, J. Heat Transf.-Trans. ASME 119 (3) 560-567, 1997.
[35] Wong, H.Y. Handbook of essential formulae and data on heat transfer for Engineers. Longman, 1977.